PROCEEDINGS OF THE ROYAL SOCIETY A

Proc. R. Soc. A (2005) **461**, 1229–1245
doi:10.1098/rspa.2004.1383
Published online 7 April 2005

Mobile assemblies based on the Bennett linkage

By Y. Chen and Z. You

University of Oxford, Oxford OX1 3PJ, UK
(zhong.you@eng.ox.ac.uk)

This paper presents a method of building large mobile assemblies using the Bennett linkage. The method is based on a basic single-layer layout consisting of overlapping $4R$ loops, each of which is a Bennett linkage. The assemblies created have a single degree of freedom, and are overconstrained and scaleable, allowing unlimited extension by repetition. In general, they deploy into a circular or non-circular cylindrical profile. The joints of the assemblies move spirally on the surface during deployment. Under some particular geometrical conditions, the profiles of the assemblies can become arch-like or flat. Moreover, the single-layer assemblies can be extended to form multi-layer mechanisms, even mobile masts. The paper shows the great versatility of the Bennett linkage and demonstrates that the century-old invention can play an important role in the construction of deployable structures.

Keywords: mechanism; Bennett linkage; overconstrained; deployable structure

1. Introduction

A century ago, G. T. Bennett (FRS, 1914) published a paper entitled 'A new mechanism' (Bennett 1903), in which he reported the discovery of a new linkage. The linkage consists of a chain of four rigid links connected by four hinges, commonly known in the mechanical engineering literature as *revolutes*, and, therefore, it is also called a 'mobile $4R$ loop'. Common mobile $4R$ loops normally contain revolutes whose axes of rotation are either parallel to one another, or concurrent, i.e. they intersect at a point, leading to 2D or spherical $4R$ linkages, respectively. However, the new linkage is an exception. In the Bennett linkage, the axes of rotation of the revolutes are neither parallel nor concurrent.

Not only does the Bennett linkage use a minimum number of links, but it is also the only $4R$ linkage with revolute connections (Waldron 1967; Savage 1972). Hence, it has attracted an enormous amount of attention from kinematicians. Fresh contributions have continuously been made to the abundant literature concerning this remarkable $4R$ linkage. Most of the reported research work has concentrated on the mathematical description and the kinematic characters of the Bennett linkage. Bennett (1914) proved that all four hinge axes of the Bennett linkage can be regarded as generators of the same regulus on a certain hyperboliod at any configuration of the linkage. Yu (1981) found that the links of the Bennett linkage were in fact two pairs of equal and opposite sides of a line-symmetrical tetrahedron. Both the equation of the hyperboloid and the geometry

Received 26 September 2003
Accepted 20 July 2004

of the quadric surface could be obtained based on the analogy. Later, Yu (1987) reported that the quadratic surface was a sphere that passed through the vertices of the Bennett linkage. A spherical $4R$ linkage could be obtained that coincided with the spherical indicatrix of the Bennett linkage. Baker (1988) investigated the *J*-hyperboloid defined by the joint-axes of the Bennett linkage and the *L*-hyperboloid defined by the links of the Bennett linkage. He was able to directly relate three independent parameters and a suitable single joint variable of the linkage with the relevant quantities of the sphere and the two forms of hyperboloid associated with it. Huang (1997) explored the finite kinematic geometry of the Bennett linkage rather than the instantaneous kinematic geometry of the linkage. Baker (2000) paid attention to the relative motion between opposite links in relation to the line-symmetric character of the Bennett linkage and discovered that it was neither purely rotational nor purely translational at any time. Furthermore, Baker (2001) examined the axode of the motion of Bennett linkage and showed that the fixed axode of the linkage was the ruled surface traced out by the instantaneous screw axis of one pair of opposite links. He established the relationships between the ruled surface and the corresponding centrode of the linkage.

Attempts have also been made to build $5R$ or $6R$ linkages using the Bennett linkage, resulting in some fascinating $5R$ and $6R$ linkages. For example, the Goldberg $5R$ linkage (Goldberg 1943) was obtained by combining a pair of Bennett linkages in such a way that a link common to both was removed and a pair of adjacent links were rigidly attached to each other. The techniques Goldberg developed can be summarized as the *summation* of two Bennett loops to produce a $5R$ linkage, or the *subtraction* of a primary composite loop from another Bennett chain to form a syncopated linkage. Goldberg also found a set of $6R$ linkages using the same technique.

In spite of the fact that Goldberg has showed that the Bennett linkage can be used as a building block for other multi-link mechanisms, so far reported research has never gone beyond building basic $5R$ and $6R$ mobile loops, except for an unsuccessful attempt by Baker & Hu (1986) to construct an assembly made from two Bennett linkages.

The aim of this paper is to explore the possibility of constructing large mobile assemblies using the Bennett linkage. These assemblies are overconstrained, have a single degree of freedom and can be used as deployable structures.

Deployable structures are a unique type of engineering structure whose geometry can be altered to meet practical requirements. Large aerospace structures, e.g. antennas and masts, are typical examples. Owing to their size, they often need to be packaged for transportation and expanded at the time of operation. A large number of deployable structures are assemblies of mechanisms whose mobility is retained for the purpose of deployment. The assemblies have the advantage of allowing repeated strain-free deployment. When selecting mechanisms, overconstrained geometry is often preferred because it provides extra stiffness, as most of such structures are for precision aerospace applications in which structural rigidity is one of the prime requirements. Furthermore, hinged connections are also favoured because they provide more robust performance than sliders and other types of connections.

Construction of large mobile assemblies has different priorities than traditional design of mechanisms in machinery. Kinematic characteristics such as the trajectory of mechanisms become less important. Keys to a successful concept include firstly identifying a robust and scalable building block made of simple mechanisms, and, secondly, developing a way by which the building blocks can be connected to form large assemblies while retaining the single degree of freedom. In this process, one has to ensure that the entire assembly satisfies the geometric compatibility.

Large mobile assemblies developed over the last three decades were based mostly on planar mechanisms, e.g. the foldable bar structures (You & Pellegrino 1997) and the panctruss structure (Rogers *et al.* 1993). The building blocks involve one or more types of basic planar mechanisms of single mobility. Three-dimensional mechanisms were rarely used. The reason was probably the mathematical difficulty in dealing with nonlinear geometric compatibility conditions in 3D.

In this paper, a method of constructing large mobile assemblies using the Bennett linkage is presented. The layout is as follows. First, a brief introduction of geometric properties of the Bennett linkage is given in §2. A method to form a single-layer network of Bennett linkages is presented in §3. This is followed in §4 by an extension to the method so that construction of multi-layer networks becomes possible. A summary of what has been achieved is given in §5, which concludes this paper.

2. The Bennett linkage

Figure 1*a* shows a Bennett linkage where the links are connected by revolutes, each of which has axis perpendicular to the two adjacent links connected by it. Define the *length* of a link as the distance between the axes of two neighbouring revolutes, the *twist* as the skewed angle between the axes of two revolutes at the ends of a link and the *offset* as the distance between the points where two adjacent links intersect with the axis of their common revolute. The conditions for the linkage to have a single degree of mobility are as follows (Beggs 1966).

– Two alternative links have the same length and the same twist, i.e.

$$a_{12} = a_{34} = a \quad a_{23} = a_{41} = b, \tag{2.1}$$

$$\alpha_{12} = \alpha_{34} = \alpha \quad \alpha_{23} = \alpha_{41} = \beta. \tag{2.2}$$

– Both the lengths and twists should satisfy

$$\frac{\sin\alpha}{\sin\beta} = \frac{a}{b}. \tag{2.3}$$

– All of the offsets are zero, i.e.

$$R_i = 0 \quad (i = 1, 2, 3, 4). \tag{2.4}$$

Values of the revolute variables, θ_1, θ_2, θ_3 and θ_4, vary when the linkage articulates. Denote θ_1 and θ_2 as θ and φ, respectively. There are

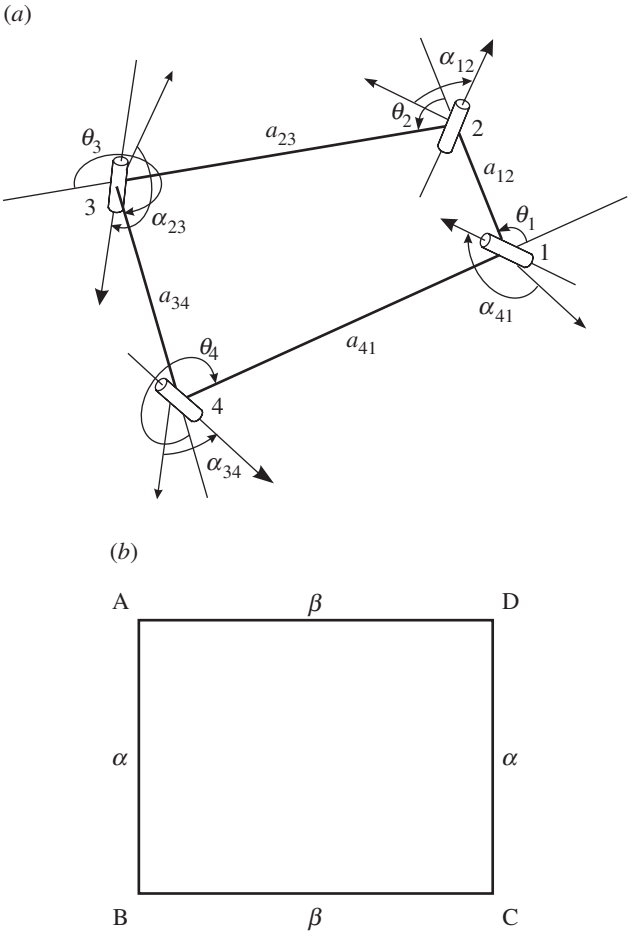

Figure 1. (*a*) A Bennett linkage. (*b*) A schematic of the linkage.

$$\theta_3 = 2\pi - \theta \quad \theta_4 = 2\pi - \varphi, \tag{2.5}$$

and

$$\tan\frac{\theta}{2}\tan\frac{\varphi}{2} = \frac{\sin\frac{1}{2}(\beta+\alpha)}{\sin\frac{1}{2}(\beta-\alpha)}. \tag{2.6}$$

Closure equations (2.5) and (2.6) ensure that only one of the revolute variables is independent, so the linkage has a single degree of mobility.

For convenience, in the next section we adopt a simpler schematic diagram shown in figure 1*b* to represent a Bennett linkage. Four links are illustrated by solid lines, and four revolute joints locate at the intersections of the lines. The twists of the joint-axes are denoted as α and β, respectively, which are marked alongside the link connecting the joints. Although the lengths of links are not marked in the diagram, it will not affect the generality as long as we bear in mind

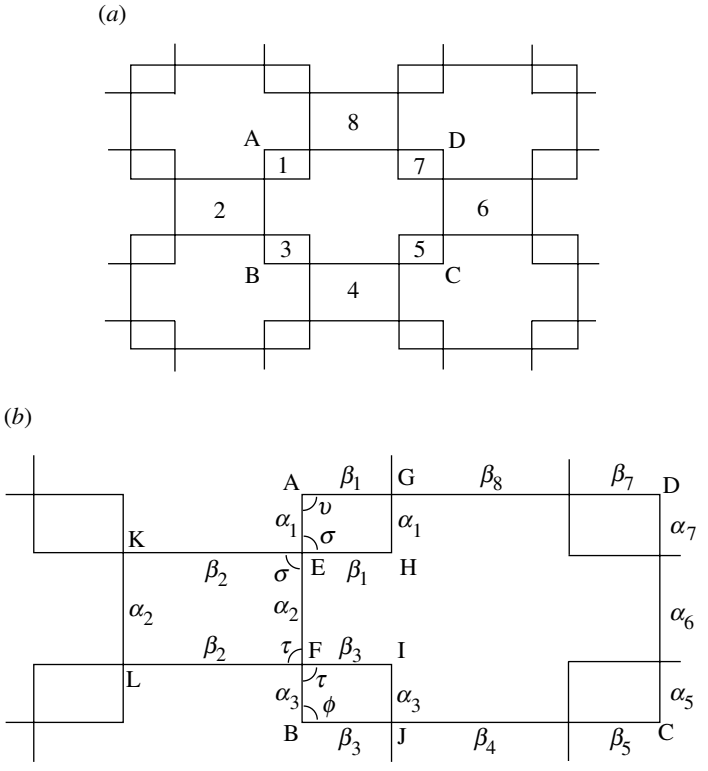

Figure 2. Single-layer network of Bennett linkages. (*a*) A portion of the network; (*b*) enlarged connection details.

that the opposite sides always have equal lengths: the horizontal and vertical ones could be a and b, respectively, or values proportional to a and b.

3. Single-layer network of Bennett linkages

A number of identical Bennett linkages with lengths a, b and twists α, β can be connected to form a network shown in figure 2*a*. A typical link in the network is represented by a straight line on which there are four revolute joints. In order to retain the single degree of mobility, it is necessary to assume that each and every $4R$ loop in the network is a Bennett linkage. While large Bennett linkage ABCD has lengths a, b and twists α, β, the smaller $4R$ loops around it, which are numbered as Bennett linkages 1–8, will have lengths a_i, b_i and twists α_i, β_i (i=1, 2, …, 8), see figure 2*b*.

Considering links AB, BC, CD and DA, there are

$$\begin{aligned} a_1 + a_2 + a_3 &= a \quad b_3 + b_4 + b_5 = b \\ a_5 + a_6 + a_7 &= a \quad b_7 + b_8 + b_1 = b \end{aligned}, \tag{3.1}$$

and

$$\begin{matrix} \alpha_1+\alpha_2+\alpha_3=\alpha & \beta_3+\beta_4+\beta_5=\beta \\ \alpha_5+\alpha_6+\alpha_7=\alpha & \beta_7+\beta_8+\beta_1=\beta \end{matrix}. \tag{3.2}$$

Let us define angles σ, τ, υ and ϕ as revolute variables, see figure 2*b*. For Bennett linkage 1,

$$\tan\frac{\pi-\upsilon}{2}\tan\frac{\pi-\sigma}{2}=\frac{\sin\frac{1}{2}(\beta_1+\alpha_1)}{\sin\frac{1}{2}(\beta_1-\alpha_1)}, \tag{3.3}$$

because of equation (2.6). Similarly, for Bennett linkages 2, 3 and ABCD,

$$\tan\frac{\pi-\sigma}{2}\tan\frac{\pi-\tau}{2}=\frac{\sin\frac{1}{2}(\beta_2+\alpha_2)}{\sin\frac{1}{2}(\beta_2-\alpha_2)}, \tag{3.4}$$

$$\tan\frac{\pi-\tau}{2}\tan\frac{\pi-\phi}{2}=\frac{\sin\frac{1}{2}(\beta_3+\alpha_3)}{\sin\frac{1}{2}(\beta_3-\alpha_3)}, \tag{3.5}$$

$$\tan\frac{\pi-\upsilon}{2}\tan\frac{\pi-\phi}{2}=\frac{\sin\frac{1}{2}(\beta+\alpha)}{\sin\frac{1}{2}(\beta-\alpha)}. \tag{3.6}$$

Combining equations (3.3)–(3.6) gives

$$\frac{\sin\frac{1}{2}(\beta_1+\alpha_1)}{\sin\frac{1}{2}(\beta_1-\alpha_1)}\frac{\sin\frac{1}{2}(\beta_3+\alpha_3)}{\sin\frac{1}{2}(\beta_3-\alpha_3)}=\frac{\sin\frac{1}{2}(\beta+\alpha)}{\sin\frac{1}{2}(\beta-\alpha)}\frac{\sin\frac{1}{2}(\beta_2+\alpha_2)}{\sin\frac{1}{2}(\beta_2-\alpha_2)}. \tag{3.7}$$

This is a nonlinear equation and many solutions may exist. By observation, two solutions can be immediately determined, which are

$$\begin{matrix} \alpha_3=\alpha & \alpha_2=-\alpha_1 \\ \beta_3=\beta & \beta_2=-\beta_1 \end{matrix}, \tag{3.8}$$

and

$$\begin{matrix} \alpha_1=\alpha & \alpha_2=-\alpha_3 \\ \beta_1=\beta & \beta_2=-\beta_3 \end{matrix}. \tag{3.9}$$

Similar analysis can be applied to Bennett linkages around links BC, CD and DA, see figure 2*a*. Based on solutions equations (3.8) and (3.9), we can conclude that twists of Bennett linkages 3, 4 and 5 should therefore satisfy

$$\begin{matrix} \alpha_3=\alpha & \alpha_4=-\alpha_5 \\ \beta_3=\beta & \beta_4=-\beta_5 \end{matrix} \quad \text{or} \quad \begin{matrix} \alpha_5=\alpha & \alpha_4=-\alpha_3 \\ \beta_5=\beta & \beta_4=-\beta_3 \end{matrix}, \tag{3.10}$$

twists of Bennett linkages 5, 6 and 7 should satisfy

$$\begin{matrix} \alpha_7=\alpha & \alpha_6=-\alpha_5 \\ \beta_7=\beta & \beta_6=-\beta_5 \end{matrix} \quad \text{or} \quad \begin{matrix} \alpha_5=\alpha & \alpha_6=-\alpha_7 \\ \beta_5=\beta & \beta_6=-\beta_7 \end{matrix}, \tag{3.11}$$

and twists of Bennett linkages 7, 8 and 1 should satisfy

$$\begin{array}{llll} \alpha_7 = \alpha & \alpha_8 = -\alpha_1 & & \alpha_1 = \alpha & \alpha_8 = -\alpha_7 \\ \beta_7 = \beta & \beta_8 = -\beta_1 & \text{or} & \beta_1 = \beta & \beta_8 = -\beta_7 \end{array}. \tag{3.12}$$

Combining the four sets of solutions given in equations (3.9)–(3.12), two common solutions, which enable the network in figure 2*a* to become mobile, are obtained:

$$\begin{array}{lll} \alpha_1 = \alpha_5 = \alpha & \alpha_2 = \alpha_4 = -\alpha_3 & \alpha_6 = \alpha_8 = -\alpha_7 \\ \beta_1 = \beta_5 = \beta & \beta_2 = \beta_4 = -\beta_3 & \beta_6 = \beta_8 = -\beta_7 \end{array}, \tag{3.13}$$

and

$$\begin{array}{lll} \alpha_3 = \alpha_7 = \alpha & \alpha_2 = \alpha_8 = -\alpha_1 & \alpha_6 = \alpha_4 = -\alpha_5 \\ \beta_3 = \beta_7 = \beta & \beta_2 = \beta_8 = -\beta_1 & \beta_6 = \beta_4 = -\beta_5 \end{array}. \tag{3.14}$$

Owing to symmetry, equations (3.13) and (3.14) are essentially the same. Thus, we take only equation (3.13) in the derivation next.

So far, only twists of each loop have been considered. Owing to equation (2.3), the corresponding lengths of each Bennett linkage must satisfy

$$\frac{\sin\alpha}{\sin\beta} = \frac{\sin\alpha_i}{\sin\beta_i} = \frac{a}{b} = \frac{a_i}{b_i} \quad (i = 1, 2, \ldots, 8). \tag{3.15}$$

A close examination of equations (3.13) and (3.15) reveals the rules governing the order of distribution of Bennett linkages within a mobile network. Diagonally, from top left corner to bottom right, there are two types of rows of Bennett linkages, see figure 3*a*. The first type consist of Bennett linkages with lengths proportional to a and b, and twists being α and β, which are denoted as 'B' in figure 3*a*. The second type, next to the first one, are made of Bennett linkages with lengths proportional to a and b, and twists being α_i and β_i or $-\alpha_i$ and $-\beta_i$, which are denoted as 'B_i' or '$-\mathrm{B}_i$' (i=1, 3, 5, ...), respectively, and both α_i and β_i satisfy equation (3.15).

A further analysis has shown that the rows of Bennett linkages in figure 3*a* marked 'B' can actually have different twists from other rows where only one type of Bennett linkage is allowed. A more general solution is given in figure 3*b* in which the Bennett linkages 'B' are replaced by 'B_j' (j=2, 4, 6, ...). A very interesting pattern now emerges: diagonally, from top left to bottom right, each row of the Bennett linkages belong to the same type. This leads to the following important feature: if a set of straight and parallel guidelines are drawn diagonally from top left to bottom right, each of which passes through a number of revolutes, these lines remain straight and parallel to each other during deployment, though the distance between the guidelines may vary during deployment of the assembly.

In general, the network shown in figure 3*b* deploys into a *cylindrical* profile. Throughout deployment, the joints forming those parallel guidelines remain straight. They expand along the longitudinal direction of the cylinder. In the other diagonal direction, i.e. the direction from top right to bottom left, joints generally deploy *spirally* on the surface of a cylinder. Figure 4 shows the deployment sequence of a mobile network model.

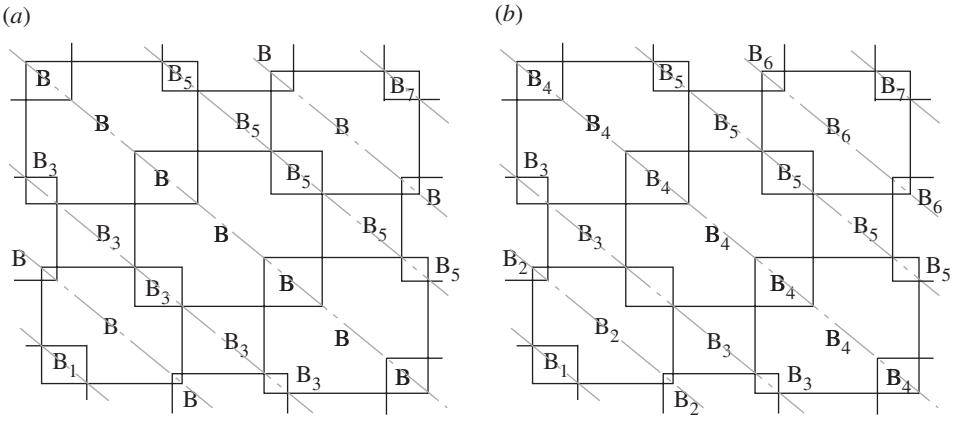

Figure 3. Mobile networks of Bennett linkages with guidelines. (*a*) A simple case; and (*b*) a more general case.

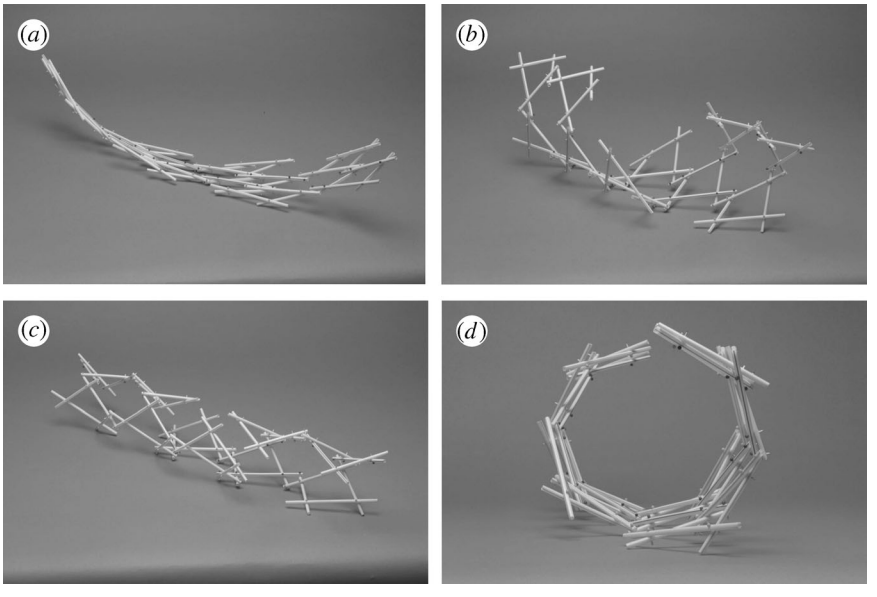

Figure 4. Example of a single-layer network of Bennett linkages. (*a*)–(*c*) Deployment sequence; (*d*) cross-sectional view of the network.

Note that we use the term *diagonal* loosely here as it is only meaningful in the schematic diagrams. In 3D, they are not obvious, and in particular, two diagonal directions are not perpendicular to each other.

The radius of curvature of the cylinder inscribed on the network depends on the values of the lengths and twists of links of each Bennett linkage and the deployment angle of the network. For instance, for the model shown in figure 4, where the lengths and twist of links are

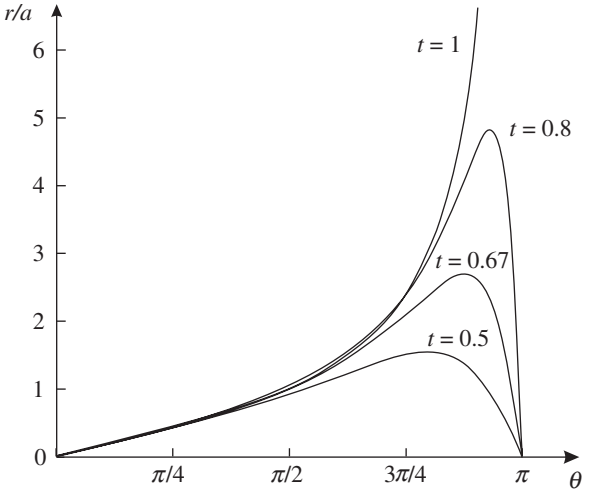

Figure 5. r/a versus θ for different t, where $t = a/b$.

$$a_i = \frac{a}{3} \quad b_i = \frac{b}{3} \quad (i = 1, 2, \ldots, 8), \tag{3.16}$$

$$\begin{aligned} &\alpha_1 = \alpha_5 = \alpha \quad \alpha_2 = \alpha_4 = -\alpha_3 = \alpha \quad \alpha_6 = \alpha_8 = -\alpha_7 = \alpha \\ &\beta_1 = \beta_5 = \beta \quad \beta_2 = \beta_4 = -\beta_3 = \beta \quad \beta_6 = \beta_8 = -\beta_7 = \beta \end{aligned}. \tag{3.17}$$

The radius of its deployed cylinder, which inscribes the network, is

$$r = \frac{t \sin\theta}{1 + t^2 + 2t\cos\theta} \sqrt{-\left(1 + t^2 + 2t\frac{1 + \cos\theta\cos\varphi}{\cos\theta + \cos\varphi}\right)}\, a,$$

where $t = b/a$, θ and φ are deployment angles of the large $4R$ loop, whose link lengths are a and b, related by equation (2.6).

When $\alpha = \pi/4$, the relationship between deployment angle, θ, and unit radius, r/a, is plotted in figure 5.

It is interesting to note that, further to equations (3.16) and (3.17), if all of the link lengths are the same, i.e. $a = b$, the network expands only *circumferentially*, forming a circular arch as shown in figure 6. Moreover, if the twists become

$$\begin{aligned} &\alpha_1 = \alpha_5 = \alpha \quad \alpha_2 = \alpha_4 = -\alpha_3 = -\alpha \quad \alpha_6 = \alpha_8 = -\alpha_7 = -\alpha \\ &\beta_1 = \beta_5 = \beta \quad \beta_2 = \beta_4 = -\beta_3 = -\beta \quad \beta_6 = \beta_8 = -\beta_7 = -\beta \end{aligned}, \tag{3.18}$$

then the network becomes a flat grid and remains flat during the deployment.

4. Multi-layer network of Bennett linkages

The network of Bennett linkages presented so far does not have overlapping layers. A typical basic unit of single-layer network of Bennett linkages is redrawn as figure 7*a*. Again the twists are marked alongside the links.

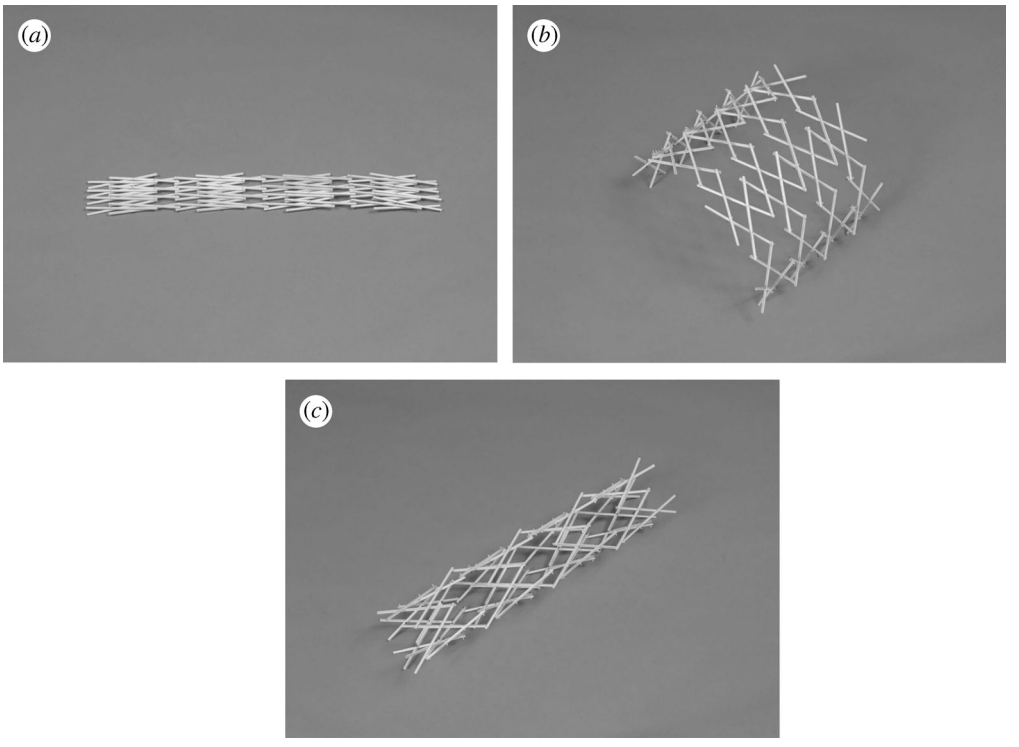

Figure 6. (*a*)–(*c*) Deployment sequence of a deployable arch.

Now let us examine whether the top right small $4R$ loop PVND can be connected with the bottom left $4R$ loop JBKS to form an assembly shown in figure 7*b*, while retaining mobility. The following proof shows that this is possible if all of the $4R$ loops are Bennett linkages.

The deployable angles and twists for each of the loops are given in figure 7*b*. Thus, the following relationships must hold.
For $4R$ loop ABCD,

$$\tan\frac{\pi-\upsilon}{2}\tan\frac{\pi-\sigma}{2}=\frac{\sin\frac{1}{2}(\beta+\alpha)}{\sin\frac{1}{2}(\beta-\alpha)}. \tag{4.1}$$

For $4R$ loop JBKS,

$$\tan\frac{\pi-\upsilon}{2}\tan\frac{\pi-\tau}{2}=\frac{\sin\frac{1}{2}(\beta_3+\alpha_3)}{\sin\frac{1}{2}(\beta_3-\alpha_3)}. \tag{4.2}$$

For $4R$ loop PVND,

$$\tan\frac{\pi-\upsilon}{2}\tan\frac{\pi-\tau}{2}=\frac{\sin\frac{1}{2}(\beta_7+\alpha_7)}{\sin\frac{1}{2}(\beta_7-\alpha_7)}. \tag{4.3}$$

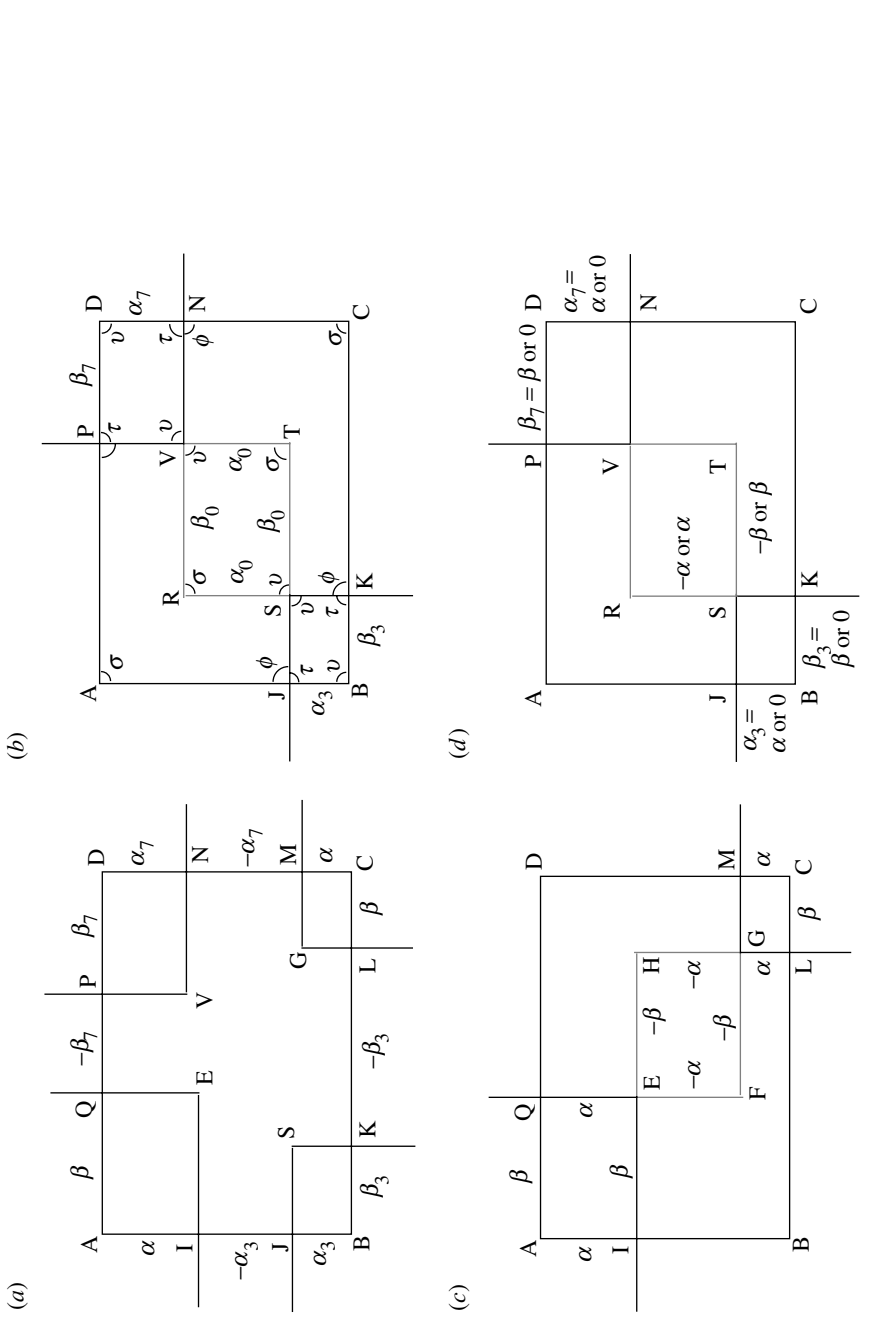

Figure 7. Formation of multi-layer mobile units. Each straight line still represents one rigid link despite variation of shades. (*a*) A basic mobile unit in a single-layer network; (*b*) formation of a multi-layer unit where loop RSTV is at a layer different from loop ABCD; and (*c*) and (*d*) two solutions leading to mobile multi-layer units.

For $4R$ loop RSTV,

$$\tan\frac{\pi-\upsilon}{2}\tan\frac{\pi-\sigma}{2}=\frac{\sin\frac{1}{2}(\beta_0+\alpha_0)}{\sin\frac{1}{2}(\beta_0-\alpha_0)}. \tag{4.4}$$

For $4R$ loop AJTP with twists $\alpha_0+\alpha_7$, $\beta_0+\beta_3$, and variables $\pi-\phi$, $\pi-\sigma$,

$$\tan\frac{\pi-\phi}{2}\tan\frac{\pi-\sigma}{2}=\frac{\sin\frac{1}{2}((\beta_0+\beta_3)+(\alpha_0+\alpha_7))}{\sin\frac{1}{2}((\beta_0+\beta_3)-(\alpha_0+\alpha_7))}. \tag{4.5}$$

For $4R$ loop RKCN with twists $\alpha_0+\alpha_3$, $\beta_0+\beta_7$, and variables $\pi-\phi$, $\pi-\sigma$,

$$\tan\frac{\pi-\phi}{2}\tan\frac{\pi-\sigma}{2}=\frac{\sin\frac{1}{2}((\beta_0+\beta_7)+(\alpha_0+\alpha_3))}{\sin\frac{1}{2}((\beta_0+\beta_7)-(\alpha_0+\alpha_3))}. \tag{4.6}$$

From equations (4.1)–(4.6), the following relationships among the twists can be obtained:

$$\frac{\sin\frac{1}{2}(\beta+\alpha)}{\sin\frac{1}{2}(\beta-\alpha)}=\frac{\sin\frac{1}{2}(\beta_0+\alpha_0)}{\sin\frac{1}{2}(\beta_0-\alpha_0)}, \tag{4.7}$$

$$\frac{\sin\frac{1}{2}(\beta_3+\alpha_3)}{\sin\frac{1}{2}(\beta_3-\alpha_3)}=\frac{\sin\frac{1}{2}(\beta_7+\alpha_7)}{\sin\frac{1}{2}(\beta_7-\alpha_7)}, \tag{4.8}$$

$$\frac{\sin\frac{1}{2}((\beta_0+\beta_3)+(\alpha_0+\alpha_7))}{\sin\frac{1}{2}((\beta_0+\beta_3)-(\alpha_0+\alpha_7))}=\frac{\sin\frac{1}{2}((\beta_0+\beta_7)+(\alpha_0+\alpha_3))}{\sin\frac{1}{2}((\beta_0+\beta_7)-(\alpha_0+\alpha_3))}, \tag{4.9}$$

$$\frac{\sin\frac{1}{2}(\beta_3+\alpha_3)}{\sin\frac{1}{2}(\beta_3-\alpha_3)}\frac{\sin\frac{1}{2}((\beta_0+\beta_7)+(\alpha_0+\alpha_3))}{\sin\frac{1}{2}((\beta_0+\beta_7)-(\alpha_0+\alpha_3))}=\frac{\sin\frac{1}{2}(\beta_0+\alpha_0)}{\sin\frac{1}{2}(\beta_0-\alpha_0)}. \tag{4.10}$$

Two sets of solutions emerge if α, $\beta\neq 0$ or π, which are

$$\begin{aligned}\alpha_3=\alpha_7=\alpha \quad \alpha_0=-\alpha\\ \beta_3=\beta_7=\beta \quad \beta_0=-\beta\end{aligned}, \tag{4.11}$$

and

$$\begin{aligned}\alpha_3=\alpha_7=0 \quad \alpha_0=\alpha\\ \beta_3=\beta_7=0 \quad \beta_0=\beta\end{aligned}. \tag{4.12}$$

When α, $\beta=0$ or π, the network becomes a number of overlapped planar crossed isograms or planar parallelograms.

Denote the lengths of links for small Bennett linkages JBKS, PVND and RSTV as a_3, b_3, a_7, b_7 and a_0, b_0. Obviously, there must be

$$\frac{a_3}{b_3}=\frac{a_7}{b_7}=\frac{a_0}{b_0}=\frac{a}{b} \tag{4.13}$$

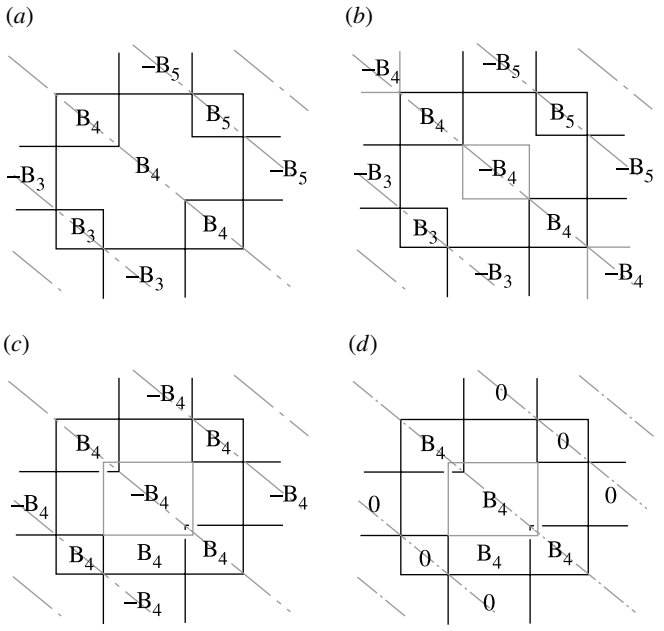

Figure 8. Construction of double layer networks of Bennett linkages. (*a*) Part of a single-layer network of Bennett linkages. (*b*) Connections along the guidelines. Grey Bennett linkages are added which form the additional layer. Connections in the other diagonal directions become possible provided that either (*c*) $B_3 = B_4 = B_5$ or (*d*) twists of B_3 and B_5 are zero. The newly added Bennett linkages are represented by grey loops and '0' represents Bennett linkages with zero twists.

and

$$a_3 + a_0 + a_7 = a \quad \text{and} \quad b_3 + b_0 + b_7 = b. \tag{4.14}$$

The solutions given in equation (4.11) mean that, in order to connect two diagonal $4R$ loops, they must have either zero twists or twists identical to those of larger $4R$ loop. Hence, the top left and the bottom right $4R$ loops can always be connected by a smaller $4R$ loop EFGH, which is at a different layer, while the top right $4R$ loop PVND and the bottom left $4R$ loop JBKS can also be connected, provided that both loops have zero twists or twists identical to those of $4R$ loop ABCD. These twists are marked alongside corresponding links in figure 7*c*,*d*.

Applying solutions equations (4.11) and (4.12) to the single-layer network shown in figure 3, a portion of which is now redrawn in figure 8*a*, yields the following conclusions:

(i) $4R$ loops denoted by even number subscripts alongside the guidelines, e.g. B_2, B_4 and B_6, etc., can always be connected by additional Bennett linkages of the same type but at a different layer forming a double layer network, see figure 8*b*.
(ii) $4R$ loops in the other diagonal direction, e.g. B_1, B_3, B_5 and B_7, etc., can be connected provided that:
   – either, twists of two smaller loops are identical to those of the loop they intend to bridge, e.g. to connect B_3 and B_5, there must be $B_3 = B_5 = B_4$, see figure 8*c*, or

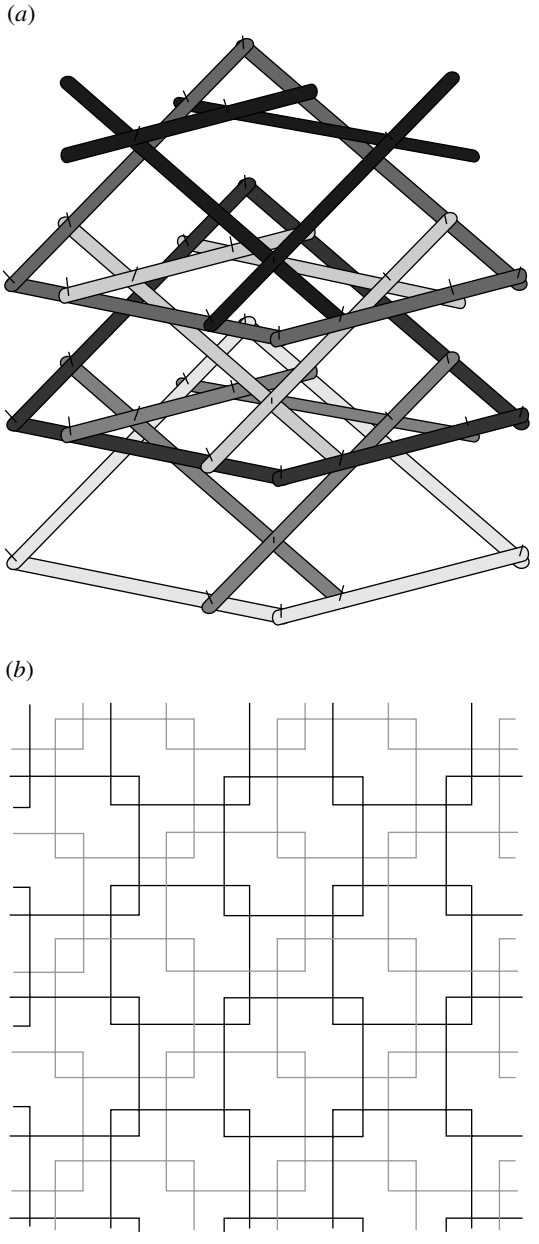

Figure 9. (*a*) A mobile mast; (*b*) another possible arrangement for multi-layer networks of Bennett linkages. Each of the squares, including those formed by two grey sides and two black sides, represents a Bennett linkage.

– twists of two smaller loops are zero, e.g. to connect B_3 and B_5, the twists of B_3 and B_5 are 0, see figure 8*d*.

Note that here, we define the equality of two Bennett linkages as both having the same twists but the link lengths being proportional to a and b.

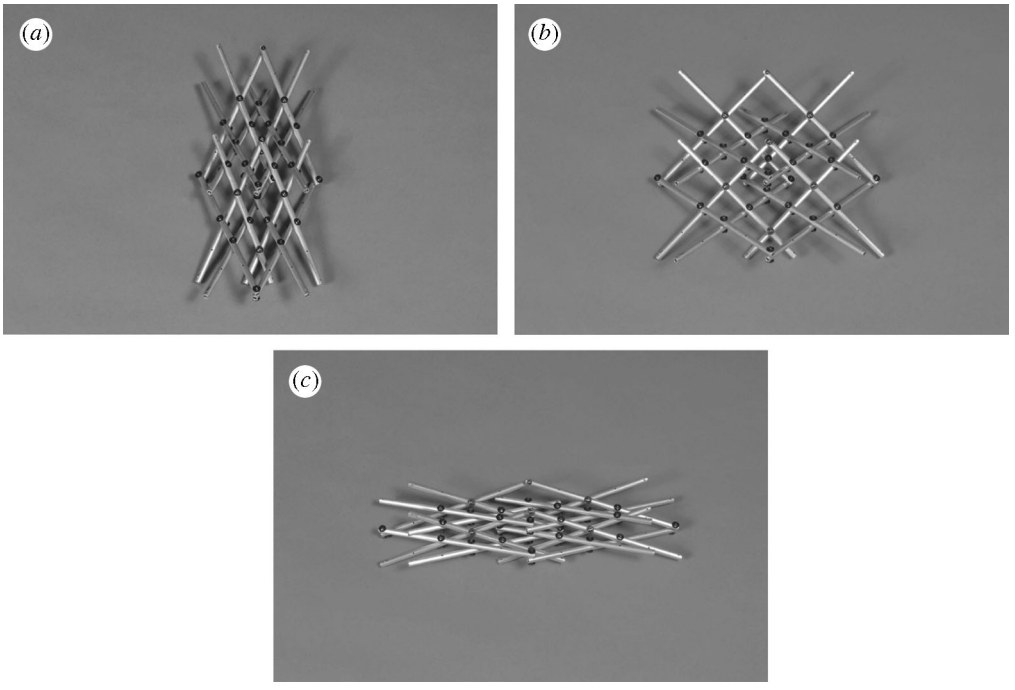

Figure 10. (*a*)–(*c*) Deployment sequence of a multi-layer network of Bennett linkages.

The networks formed using the rules above will have double layers.

Similar to a single-layer network, the solutions for forming double-layer mobile networks can be extended to build multi-layer networks by repetition. For example, consider a single unit shown in figure 7*d*. If the bridging links at the upper layer are extended, a larger Bennett linkage at a higher layer can be connected to it. The process can be repeated, resulting in the formation of a mobile multi-layer mast, see figure 9*a*. The same process can be applied laterally. Figure 9*b* shows another possible arrangement. Each of the $4R$ loops, including the ones whose sides have different shades, is a Bennett linkage. Figure 10 shows a physical model of a multi-layer mobile assembly in which links are made of Al-alloy rods. It is interesting to note that if the two smallest Bennett linkages at the centre of the model were removed, the assembly would show the largest Bennett linkage and the second largest one being connected by four smaller Bennett linkages on each side. This, effectively, provides a solution to the question of connecting two Bennett linkages that Baker & Hu (1986) raised (Chen & You 2002).

5. Conclusion

Sixty years ago, Goldberg (1943) built his $5R$ or $6R$ linkages based on the Bennett Linkage, using *summation* and *subtraction* of Bennett linkages. Now we

are able to construct a family of large mobile assemblies based on Bennett linkages with the following features:

(i) the basic layout of the assemblies consists of a single-layer network of overlapping $4R$ loops, see figure 3*b*. These assemblies are scaleable, allowing unlimited extension by repetition;
(ii) each of the $4R$ loops is a Bennett linkage;
(iii) the assemblies created are overconstrained and have a single degree of freedom;
(iv) in general, these assemblies deploy into a profile of cylindrical surface, whose cross-section may or may not be circular. The joints move spirally on the surface during deployment;
(v) under some particular geometrical conditions, the profiles of the assemblies can become arch-like or flat;
(vi) the single-layer assemblies can be extended to form multi-layer mechanisms, or mobile masts consisting of Bennett linkages.

It should be pointed out that in some basic configurations, e.g. those shown in figure 7*c*,*d*, there are also two $6R$ loops. Considering that these loops are created by a process similar to the summation and subtraction of Bennett linkages, we therefore conclude that the assemblies presented here are purely based on the Bennett linkage.

We have emphasized that the assemblies can be enlarged by repetition. However, they can also be scaled down by removing some links, revolutes or loops. This is because, first of all, the assemblies are overconstrained, and secondly, the summation and subtraction of Bennett linkages proposed by Goldberg can also be used.

It should be pointed out that the mathematical derivation does not consider the cross-sectional dimension of the links. Despite the fact that the physical models presented in this paper are made of solid rods whose cross-sectional dimension is small but finite, and there exist unavoidable errors in the manufacturing and assembling process, it has been found that these factors do not hinder the performance of the assemblies.

This research work was supported by grants from the Engineering and Physical Sciences Research Council in Britain (GR/M61207) and the Lubbock trust fund. Y.C also wishes to thank the University of Oxford, where she received a graduate scholarship.

References

Baker, E. J. 1988 The Bennett linkage and its associated quadric surfaces. *Mech. Mach. Theory* **23**, 147–156.

Baker, E. J. 2000 On the motion geometry of the Bennett linkage. *Mech. Mach. Theory* **35**, 1641–1649.

Baker, E. J. 2001 The axodes of the Bennett linkage. *Mech. Mach. Theory* **36**, 105–116.

Baker, E. J. & Hu, M. 1986 On spatial networks of overconstrained linkages. *Mech. Mach. Theory* **21**, 427–437.

Beggs, J. S. 1966 *Advanced mechanism*. New York: Macmillan Company.

Bennett, G. T. 1903 A new mechanism. *Engineering* **76**, 777–778.

Bennett, G. T. 1914 The skew isogram mechanism. *Proc. London Mathematics Society, 2nd series*, 13.

Chen, Y. & You, Z. 2002 Connectivity of Bennett linkages. *The 43rd AIAA/ASME/ASCE/AHS/ ASC Structures, Structural Dynamics and Materials Conference, Denver, CO, USA*. (AIAA 2002-1500.)

Goldberg, M. 1943 New five-bar and six-bar linkages in three dimensions. *Trans. ASME* **65**, 649–663.

Huang, C. 1997 The cylindroid associated with finite motions of the Bennett mechanism. *Trans. ASME, J. Eng. Ind.* **119**, 521–524.

Rogers, C. A., Stutzman, W. L., Campbell, T. G. & Hedgepeth, J. M. 1993 Technology assessment and development of large deployable antennas. *J. Aerospace Eng.* **6**, 34–54.

Savage, M. 1972 Four-link mechanisms with cylindric, revolute and prismatic pairs. *Mech. Mach. Theory* **7**, 191–210.

Waldron, K. J. 1967 A family of overconstrained linkages. *J. Mech.* **2**, 210–211.

You, Z. & Pellegrino, S. 1997 Foldable bar structures. *Int. J. Solids Struct.* **34**, 1825–1847.

Yu, H.-C. 1981 The Bennett linkage, its associated tetrahedron and the hyperboloid of its axes. *Mech. Mach. Theory* **16**, 105–114.

Yu, H.-C. 1987 Geometry of the Bennett linkage via its circumscribed sphere. In *Proc. 7th World Congress on the Theory of Machines and Mechanisms, Sevilla, Spain, 17–22 September*, 1, pp. 227–229.